

DETECTION OF GLIOMA EVOLUTION ON LONGITUDINAL MRI STUDIES

E. D. Angelini, J. Atif, J. Delon

E. Mandonnet, H. Duffau, L. Capelle

GET, Ecole Nationale Supérieure des
Télécommunications, CNRS UMR 5141
Paris, FRANCE

Hôpital Pitié Salpêtrière
Department of Neurosurgery
Paris, FRANCE

ABSTRACT

Detection of millimetric brain tumor growth patterns on longitudinal MRI acquisitions remains challenging in clinical practice. A simple difference map of two longitudinal co-registered MRI volumes fails to detect specific tumor evolution, due to non-linear contrast change between the two data sets. This paper presents a novel method for detection and quantification of tumor evolution in longitudinal single-protocol MRI studies. A computational framework was designed to enable comparison of co-registered MRI volumes based on gray-scale "normalization" via midway histogram equalization and computation of difference maps. Midway-based difference maps provided very selective representations of structural modifications within pathological areas and on the surrounding structures. Quantitative tumor growth parameters between times t_1 and t_2 were computed on the difference maps, provided that a manual segmentation of the tumor is available at time t_1 . The method was evaluated on longitudinal SPGR (T1-weighted) and FLAIR (T2-weighted) MRI volumes for two patients harboring a WHO grade II glioma. Results for quantification of tumor growth from midway difference maps are presented, showing sub-millimetric precision of clinical growth indices, when compared to manual tracing estimations.

keywords: Biomedical imaging, magnetic resonance imaging, brain tumor, longitudinal studies.

1. INTRODUCTION

It has been recently shown that quantitative measurements of glioma dynamics is crucial for the therapeutic management of these tumors [1]. Detection of a small increase (or decrease) in brain tumor volume on longitudinal MRI exams remains challenging and current standard methods compare manually segmented tumors at follow up times. However, manual segmentation is a time consuming task, rarely performed in clinical practice. Moreover, inter-observer variability for manual tracing of brain tumor can range up to 15% [2]. Automated algorithms for brain tumor segmentation may be helpful, but lack reliability for infiltrative grade II glioma [2]. In addition, long-term post-operative images exhibits regions of abnormal signals hard to classify by segmentation algorithm. A differ-

This project was funded by GET and INCA grants. J. Atif is now with Université des Antilles et de la Guyane, Guyane, FRANCE. H. Duffau is now with the Hpital Gui de Chaumiery, CHU de Montpellier, FRANCE.

ence map of two successive co-registered MRI would constitute the simplest approach to detect small changes in tumor size, but is not applicable due to very different gray-level and contrast ranges between two MRI volumes. In this paper, we propose to perform a non-linear gray-level normalization of the two successive MRI scans, enabling difference map computation and voxel-based quantification of the tumor evolution.

2. METHOD

2.1. MRI Studies

Clinical monitoring of a patient's tumor evolution is routinely performed via MRI scanning of the patient's brain at regular time intervals (t_1, t_2, \dots), with SPGR (T1-weighted) and FLAIR (T2-weighted) protocols. Typical spatial resolutions for the MRI volumes used in this study were $(0.9 \times 0.9 \times 1.5)$ mm³ for SPGR protocol and $(0.9 \times 0.9 \times 6.5)$ mm³ for the FLAIR protocol. FLAIR and SPGR data sets from time $t_n, n > 1$ were independently registered to time t_1 , as detailed in Section 3.

Gray-level dynamic range of SPGR and FLAIR data sets can vary greatly between two scanning sessions, partly due to specific parameter settings for MRI data reconstruction from the acquired K-space. Longitudinal comparison methods need to be insensitive to typical scanning differences, including head position, scanner noise, dynamic range and voxel size, while being able to detect biological evolutions of the tumor (and eventually modification of other cerebral brain structures) depicted as morphological or signal changes.

To illustrate the challenges raised by longitudinal scan comparison, we computed in Figure 1 difference maps from direct subtraction of two SPGR MRI volumes. Linear intensity range mapping was performed via rescaling voxel values to an 8-bits range or to an intermediate range between the half minimum and half maximum values from the two scans. We observed here that direct difference maps did not provide specific information related to the tumor evolution, and included anatomical information due to global differences in tissue gray levels. This suggests that linear gray-scale mapping is not sufficient to bring longitudinal MRI scans into a common gray-scale range of values permitting direct comparison and motivated our work to derive non-linear mapping of MRI scans based on midway histogram equalization as detailed in the fol-

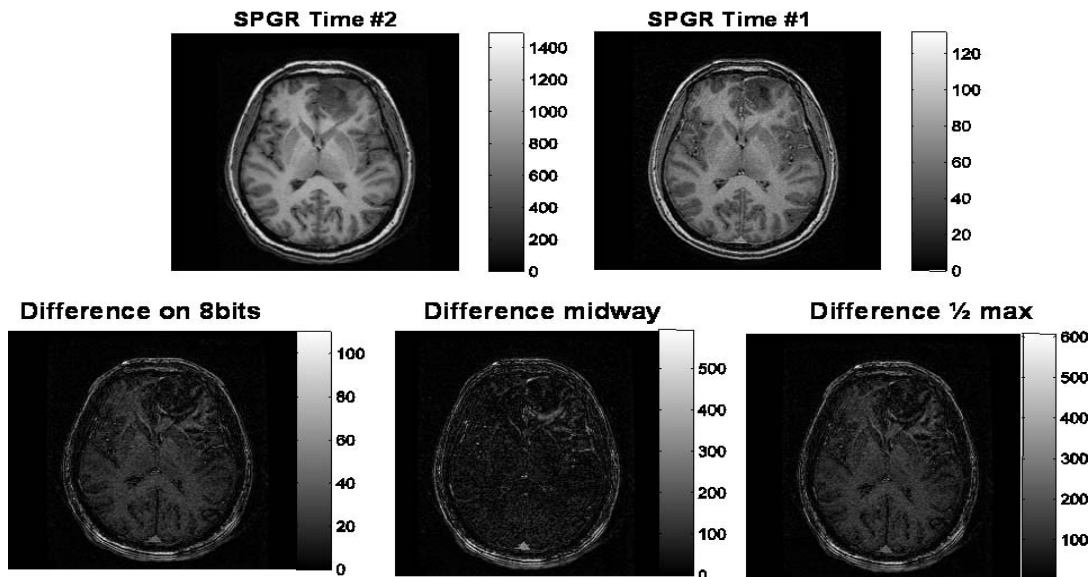


Fig. 1. Illustration of difference maps between two SPGR MRI volumes

lowing sub-Section.

2.2. Midway Image Equalization

Midway image equalization consists of the derivation of a fitting function to map a pair of images by bringing their histogram to a similar shape. Such image transform, is part of a more global family of histogram specification transforms. Several of these transforms exist, with varying performance in terms of preservation of the original dynamic range. In the general framework, transformation of an image I , with cumulative histogram H , via a mapping function $\varphi : [0, 1] \rightarrow [0, 1]$ creates an image with cumulative histogram $H_t = H \circ \varphi^{-1}$. Classical applications of image histogram specification include histogram equalization where the target cumulative histogram H_t is the identity function, and histogram mapping where H_t is the cumulative histogram of a target image I_t .

A more sophisticated problem arises when one is interested in an "average" representation of two images I_1 and I_2 with H_t being a compromise between H_1 and H_2 . In this context, Delon in [3] recently proposed two methods to derive such "averaging", or midway mapping function, based on an axiomatic analysis of the image equalization process. This approach enforces robust behavior of the mapping process in when the two images differ by a constant value or by a contrast change. In the second case, it is assumed that there exists an image I and two increasing contrast functions f and $g : [0, 1] \rightarrow [0, 1]$ so that $I_1 = f(I)$ and $I_2 = g(I)$. In that case, it can be shown that the only intermediate mapping between the two images which provides a direct averaging, independent of the contrast functions is defined by $H_t = \left(\frac{H_1^{-1} + H_2^{-1}}{2} \right)^{-1}$, which is called the inverse average equalization. This result

is the continuous version of the dynamic histogram warping from Cox *et al.* [4]

In our case, we were interested in comparing MRI scans from a single patient and a single MRI protocol but acquired at different time intervals. For a healthy patient, the two co-registered scans represent the exact same anatomy but might differ in terms of contrast, due to different scanning and acquisition set ups. For a patient with a localized evolving pathology, such as a tumor, the MRI scans should represent approximately the same anatomy, except around the pathological site, where structural changes and image contrast modifications might occur. If the evolution of the pathology involves only small modifications, differences between the two scans can be viewed as a global contrast change with minor localized structural modifications that will not affect the cumulative histogram (i.e. cumulative frequencies of voxel values). In such case, midway image equalization is well suited to bring the two MRI scans into a common range of gray values and allow direct image data comparison via difference maps.

2.3. Implementation of Midway Equalization

Given two longitudinal MRI scans I_1 and I_2 from a single protocol, we first computed the cumulative histograms H_1 and H_2 , accumulating frequency values associated with increasing gray levels found in the data. These histograms need to be inverted to compute H_1^{-1} and H_2^{-1} . During the inversion process, arbitrary assignments have to be made for gray levels with similar cumulative occurrences (i.e. assign cumulative frequencies to missing gray values within the dynamic range of the data). Two strategies have been tested via nearest neighbor or linear interpolation of the gray values assigned to successive cumulative frequency bins, leading to similar results.

After cumulative histograms inversion, an average cumulative histogram was computed, along with the mapping function that will bring I_1 and I_2 to an average gray-level range of values. Histogram computations and inversions were performed in less than a minute for two MRI data volumes, on a regular Linux PC workstation.

2.4. Detection and Quantification of Tumor Growth

A difference map was computed by direct subtraction of the midway equalized MRI scans, as illustrated in Figure 1. This difference map provided a sparse representation of the scans differences with high values corresponding to the evolving parts of the tumor. Small pieces of tissue edges could also be recognized on the difference map, corresponding to local shape modifications of some anatomical structures, such as the lateral ventricle on the tumor’s side, as well as minor residual registration errors. This difference map therefore needed to be cleaned up to enable specific quantification of the pathological evolution.

Post-processing of the midway difference map was performed via clustering of the difference values into two classes. The smallest cluster was preserved, which corresponded to a small subset of high difference values. A region of interest (ROI) was defined via dilation of the tumor’s shape, manually segmented at time t_1 . Connected components of the preserved cluster, overlapping with the ROI were extracted and tested in terms of homogeneity of their difference values. Any connected component with a bi-modal histogram (for SPGR) or with low average intensity values (for FLAIR) was removed. This step was required to avoid the inclusion of high difference values generated on the skull due to mis-registration errors, and on the CSF lateral ventricles, due to additional mass-effects from the expanding tumor.

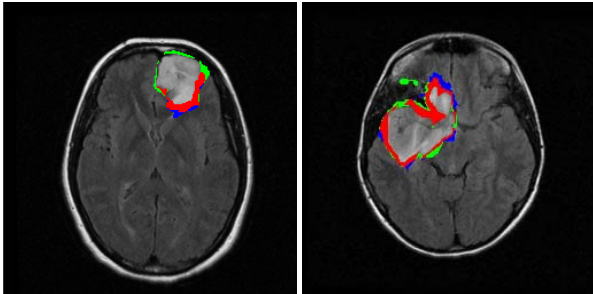


Fig. 2. Tumor growth measured on FLAIR data via midway-based difference maps or manual tracing: colors correspond to agreeing (red), manual extra growth (green), and midway-based extra growth (blue) parts.

3. RESULTS

Midway-based tumor growth quantification was evaluated on two patients with low-grade gliomas (Patient 1 included pre-

surgical data, Patient 2 included post-surgical data), respectively screened at 5 and 10 months intervals (interval times between t_1 and t_2), with SPGR and FLAIR protocols. Manual tracing of the tumor was performed on both protocols at both screening times (i.e. 4 manual segmentations per patient) with the free software package MRICro. Registration of single-protocol longitudinal MRI scans and their associated manual segmentation was performed with the free software package FSL, using mutual information, affine transformations and nearest neighbor interpolation. Manual growth estimation was performed by simple binary difference between the two manual tracings, for individual protocols. Midway equalization was run separately on the SPGR and FLAIR protocols and automated detection of significant changes within an ROI defined from manual tracing at time t_1 was performed. Illustrations of the agreement between manual and midway growth patterns is illustrated in Figure 2 for the two clinical cases. Illustrations of 3D tumor shapes and growth from SPGR and FLAIR scans of the left case in Figure 2 are provided in Figure 3 .

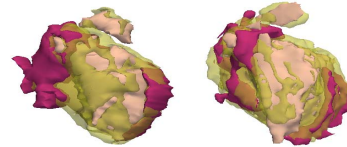


Fig. 3. Visualization of 3D tumor growth on SPGR (left) and FLAIR (right) with manual tracing (green) and midway-based differences (pink)

Quantitative measurements were performed on the tumor growth patterns as reported in Table 1. Tumor growth volumes in *ml* and standard growth error measurements including true positive (TP), false negative (FN) and false positive (FP) volume fractions(VF) were computed. Then growth indices were computed, including volume percentage increase. Linear growth rate of mean tumor diameters, of prognosis interest in clinical practice [1], was also computed as the radius increase of the sphere with volume equal to the tumor’s one.

		Growth Overlap						Growth Indices					
SPGR	FLAIR	TP VF (%)		FP VF (%)		FN VF (%)		volume (ml)		volume %		Radius (mm)	
		#1	Manual							14	13	36	29
	Midway	53	65	47	35	41	12	16	18	40	40	1.0	1.0
#2	Manual							18	19	41	36	1.0	1.0
	Midway	50	57	50	43	61	31	14	24	33	43	0.8	1.2

Table 1. Quantitative comparison of tumor growth assessed on SPGR and FLAIR data.

Even though volume and overlap measures were not very accurate, differences in sphere-equivalent radius increase, as

measured by the two methods, remained below 1mm , which is below voxel resolutions. More over, FLAIR measurements seemed slightly more accurate in terms of growth volume overlap, corroborating the well known fact that it is easier and more reliable to segment grade II glioma on FLAIR than on T1-weighted MRI data.

4. DISCUSSION AND CONCLUSIONS

In this study, we presented a novel method for midway-based comparison and quantification of tumoral evolution on longitudinal MRI studies that generated very accurate clinical growth index measurements on two patients. Midway equalization of MRI scans enabled the computation of very selective difference maps, robust to disparities in the dynamic range of the MRI data sets being compared.

Some concerns remain regarding the influence of the registration quality on the overall tumor growth quantification. Brain tumors can induce significant modifications on the surrounding cerebral structures such as the lateral ventricles, due to tumor mass-effect. These cerebral structures contribute to the alignment optimization process performed during registration of the longitudinal MRI scans. Recent registration works have focused on developing specific methods for brain MRI data with tumors [5]. It is very likely that future use of dedicated registration methods could greatly improve the selectivity of the difference maps computed after midway equalization.

Midway brain MRI equalization provided a very efficient computational framework for gray scale "standardization". In [6], Nyul *et al.* proposed a piecewise linear histogram transformation, to map a "model" shape defined with landmark points corresponding to percentile levels and median values, whose positions were learned on a training database of MRI images. In our framework, issues related to the use of average landmark points and their unknown "anatomical" significance was avoided with the global midway equalization transform. We could investigate the effect of gray-value quantification on the midway-based difference map selectivity. A recent exact histogram specification method was proposed by Coltuc *et al.* in [7], ordering all image pixels depending on their gray levels and local averages. In our case, limitations would arise from the high computational cost of 3D pixel ordering and the use of an image-dependent pixel ordering that cannot preserve the overall hierarchy of tissue intensity, in two longitudinal MRI data sets that need to be compared.

Tumor growth quantification with the proposed method was directly dependent on the efficiency of the post-processing in selecting "meaningful" high values from the difference map. Different post-processing frameworks could be investigated. An interesting approach was proposed on a similar problem by Liu *et al.* [8] to select only significant changes on SPGR, T2-weighted and FLAIR longitudinal brain MRI scans. Their method used simple difference maps. First a noise level map

was created from the registration of repeated scans for a given subject. Structured difference images were then generated by thresholding the difference maps and spatially clustering growth features. Finally, the significance of the detected changes was assessed by thresholding the difference maps against an anatomical map of artifacts computed from spatial normalization of difference maps from 40 subjects. This final threshold used a probabilistic experimental level of significance. We proposed an alternative computational framework to compare single-protocol repeated scans without the need for integrating image-based noise level evaluation. Indeed the first thresholding operation was designed to remove, from the difference maps, random MRI signal variation in repeated scans due to physiological and scanner related artifacts. In our method, this correction was directly performed in the midway mapping process, eliminating the need for *ad-hoc* threshold levels that might eliminate structural differences as well.

In conclusion, this paper provided a "proof-of-concept" for a new clinical tool to detect and quantify tumor evolution on brain MRI data. This tool will be evaluated on a large series of patients with brain tumors of different grades. It is interesting to note that the method is not specific to the quantification of brain tumor evolution and could be applied to other reviewing tasks on follow-up MRI scans.

5. REFERENCES

- [1] J. Pallud, E. Mandonnet, H. Duffau, M. Kujas, R. Guillevin, D. Galanaud, L. Taillandier, and L. Capelle, "Prognostic value of initial magnetic resonance imaging growth rates for world health organization grade II gliomas," *Annals of Neurology*, vol. 60(3), pp. 380–383, 2006.
- [2] M. R. Kaus, S. K. Warfield, A. Nabavi, P. M. Black, F. A. Jolesz, and R. Kikinis, "Automated segmentation of MR images of brain tumors," *Radiology*, vol. 218, pp. 586–591, 2001.
- [3] J. Delon, "Midway image equalization," *Journal of Mathematical Imaging and Vision*, vol. 21(2), pp. 119–134, 2004.
- [4] I.J. Cox, S. Roy, and S.L. Hingorani, "Dynamic histogram warping of image pairs for constant image brightness," in *IEEE International Conference on Image Processing*, Washington, DC, USA, feb 2006, vol. 2, pp. 366–369.
- [5] O. Clatz, H. Delingette, I.-F. Talos, A.J. Golby, R. Kikinis, F.A. Jolesz, N. Ayache, and S.K. Warfield, "Robust nonrigid registration to capture brain shift from intraoperative MRI," *IEEE Transactions on Medical Imaging*, vol. 24(1), 2005.
- [6] L. G. Nyul, J. K. Udupa, and X. Zhang, "New variants of a method of MRI scale standardization," *IEEE Transactions on Medical Imaging*, vol. 19(2), pp. 143–150, 2000.
- [7] D. Coltuc, P. Bolon, and J.-M. Chassery, "Exact histogram specification," *IEEE Transactions on Image Processing*, vol. 15-5, pp. 1143–1152, 2006.
- [8] R. S. N. Liu, L. Lemieux, G. S. Bell, S. M. SisoDiya, S. D. Shorvon, J. W. A. S. Sander, and J. S. Duncan, "A longitudinal study of brain morphometrics using quantitative magnetic resonance imaging and difference image analysis," *NeuroImage*, vol. 20, pp. 22–33, 2003.